

# Expert Opinion

1. Introduction
2. Types of drug delivery carrier geometries
3. Drug loading, stability and release
4. Circulation
5. Targeting
6. Cellular uptake and subcellular trafficking
7. Conclusion
8. Expert opinion

## Polymeric carriers: role of geometry in drug delivery

Eric A Simone<sup>†</sup>, Thomas D Dziubla & Vladimir R Muzykantov<sup>†</sup>

<sup>†</sup>University of Pennsylvania, Philadelphia, PA 19104, USA

The unique properties of synthetic nanostructures promise a diverse set of applications as carriers for drug delivery, which are advantageous in terms of biocompatibility, pharmacokinetics, targeting and controlled drug release. Historically, more traditional drug delivery systems have focused on spherical carriers. However, there is a growing interest in pursuing non-spherical carriers, such as elongated or filamentous morphologies, now available due to novel formulation strategies. Unique physiochemical properties of these supramolecular structures offer distinct advantages as drug delivery systems. In particular, results of recent studies in cell cultures and lab animals indicate that rational design of carriers of a given geometry (size and shape) offers an unprecedented control of their longevity in circulation and targeting to selected cellular and subcellular locations. This article reviews drug delivery aspects of non-spherical drug delivery systems, including material selection and formulation, drug loading and release, biocompatibility, circulation behavior, targeting and subcellular addressing.

**Keywords:** Formulation, geometry, micelle, nano, polymer

*Expert Opin. Drug Deliv.* (2008) 5(12):1283-1300

### 1. Introduction

In recent years, the drug delivery field has experienced an exponential growth of interest in the role played by the carrier's geometry (i.e., shape and size) in its functions – drug loading and release, stability, toxicity and, ultimately, delivery performance. Intuitively, one could *a priori* postulate that the geometry governs the carrier's behavior *in vivo*: circulation and elimination, permeation into, retention in and clearance from tissues, interaction with target cells and subcellular trafficking and final addressing of a cargo. Biology provides numerous examples of the key role of geometry in transporting features of large spherical leukocytes, small spherical lipoproteins, large discoid erythrocytes, small discoid platelets, and rod-like and filamentous microbes of diverse size. Alas, the limitations of the previous methods to vary and control the geometry of drug delivery systems (DDS) did not favor systematic experimental efforts in this area of research. Most DDS designed in the last three decades have either spherical (e.g., liposomes, dendrimers and micelles) or irregular morphology (protein conjugates, linear backbone polymer conjugates, polyplexes). However, the development of methods for formulation and characterization of polymeric drug carriers enabled design of carriers with versatile and defined geometries. This article represents an attempt to systematically analyze the rapidly growing body of experimental data obtained *in vitro* and in animal studies using carriers of diverse morphologies and geometries.

### 2. Types of drug delivery carrier geometries

There is an immense body of literature on spherical carriers, varying in size from a few nanometers (quantum dots, small micelles and dendrimers) to 50 – 500 nanometers (liposomes, polymer carriers, large dendrimers, lipoproteins)

**informa**  
healthcare

to microns (blood cells and polymer carriers). Any attempt to review these carriers would be unrealistic; in this paper they will be discussed mainly as a comparison group with non-spherical carriers of corresponding size. Non-spherical carriers discussed in this paper include anisotropic polymer particles such as flat nanodisks, molded nanocubes or cylinders, elongated liposomes, filamentous polymer micelles ('filomicelles', also referred to as 'worm micelles'), filamentous polymer nanocarriers and carbon nanotubes. Schematics of these geometries are depicted in Figure 1.

From the standpoint of size, many of these carriers, traditionally called 'nanocarriers', exceed the National Science Foundation (NSF) dimensional limits defined for 'nanoscale' (< 100 nm), yet fit within broader nanoscale definitions (< 1,000 nm). Furthermore, the term *nanostructure* refers to any non-spherical carrier with at least one dimension that is less than one micron, typically less than 100 nm.

The unique physical, chemical and optical properties of nanostructures hold promise for a variety of applications in drug delivery. By virtue of their small size, nanoscale materials offer distinctive advantages including unique pharmacokinetics (see sections 4 and 5, below). From a geometric argument, *nano* carriers have an enormous surface area to volume ratio, favoring surface conjugation of functional moieties. In terms of stability, reduction of carrier dimensions to the nanoscale can enhance water penetration and thus degradation of biodegradable carriers (see Section 3). Due to their relatively low density and the unique combination of electrostatic and van der Waal surface forces relevant at this size scale, nanoparticles tend to stay in solution without extensive sedimentation, thus extending their biomedical utility, compared to larger carriers. Furthermore, nanoscale is more conducive to effective transport functions *in vivo*, both in the circulation and at the subcellular level (see Sections 4 and 6).

## 2.1 Spheroid nanocarriers

The most basic and common geometry of nano DDS is spherical. On the smaller side, diameters of these DDS range from 50 – 300 nm liposomes [1], polymersomes [2] (the synthetic analog of a liposome), dendrimers and polyplexes [3], to ~ 5 – 50 nm gold [4], silica [5], or iron oxide [6] nanoparticles and semiconductor crystals, or quantum dots, used as the core of dual-imaging/treatment DDS [7]. On the intermediate and larger side, some DDS exceed the NSF definition of nanoscale, but still possess many of the beneficial properties of their *nano* counterparts. Such submicron DDS include 300 – 1000 nm diameter polymer spheroids [8]. Polystyrene spheroids that span the size range from sub-100 nm to several microns have been utilized to explore cellular mechanisms of nanoparticle DDS uptake and processing [9,10]. They have also been used to study their circulation when coated with proteins [11] or coupled to erythrocytes to extend their *in vivo* circulation half life [12].

## 2.2 Elongated liposomes

Perhaps one of the most extensively studied carriers in drug delivery, liposomes are traditionally thought of as spherical vesicles composed of amphiphilic phospholipids, but this category also includes non-spherical structures. One of the earliest studies mixed lysolecithin with phospholipids to produce disc, cylindrical and elongated rod-like micelles [13]. Other examples of non-spherical liposomes include tubules, cochleate cylinders and ribbons. Tubules, elongated hollow/water-filled cylinders formed from phospholipids by cooling them below their chain melting transition temperature [14], protected labile drug cargoes from proteolytic degradation [15]. Cochleate (snail-like, spirally twisted) cylindrical particles typically consist of common liposomal reagents such as phosphatidylserine that are negatively charged before precipitation by a cation such as calcium [16]. Another non-spheroid liposome-based structure is the ribbon-shaped particle formed by complexation of amphotericin B, an antifungal antibiotic, and lipids in specific ratios [17]. Some groups have applied electric fields to stretch liposomes into elongated nanotubules [18].

## 2.3 Flattened nanocarriers

A large class of non-spherical model drug carriers is constructed of non-biodegradable polystyrene, formed into diverse geometries including flat elliptical disks and rods, among other non-traditional shapes. The versatility of their geometries affords interesting insights into the role of shape in drug delivery [11,19], some of which shall be discussed in subsequent sections of this review. For elliptical disks, dimensions can be in the order of 10 – 20 microns on the major axis, while the height ranges from 100 to 1000 nm. Other shapes include, but are not limited to, rectangular disks, rods, worms, oblate ellipses, flat circular disks, barrels, bullets, pills, pulleys, ribbons with curled ends, bicones and UFOs (as in the sci-fi *flying saucer*) [20]. Fabrication is relatively simple and utilizes approaches for similarly shaped particles for other applications, that is immobilization of polystyrene spheres onto a polymer substrate, before heating above the glass transition temperature of the polystyrene and mechanical stretching of the substrate [20,21]. Conditions are easily manipulated, such as stretching in air versus in a solvent, to control the ultimate particle geometry. After the mechanical manipulation stage, the immobilizing polymer film is dissolved, releasing the stretched particles. This technique can be extended to degradable PLGA polymer particles, yet the utility of this formulation – material combination has yet to be fully realized [22].

## 2.4 Micro/nano fabricated nanocarriers

Another approach to control carrier geometry on the nanometer – micron length scale comes from micro/nanofabrication techniques. Some of the earlier studies utilized either microfluidics to form emulsions [23] or combinations of microfluidics and microscope projection photolithography

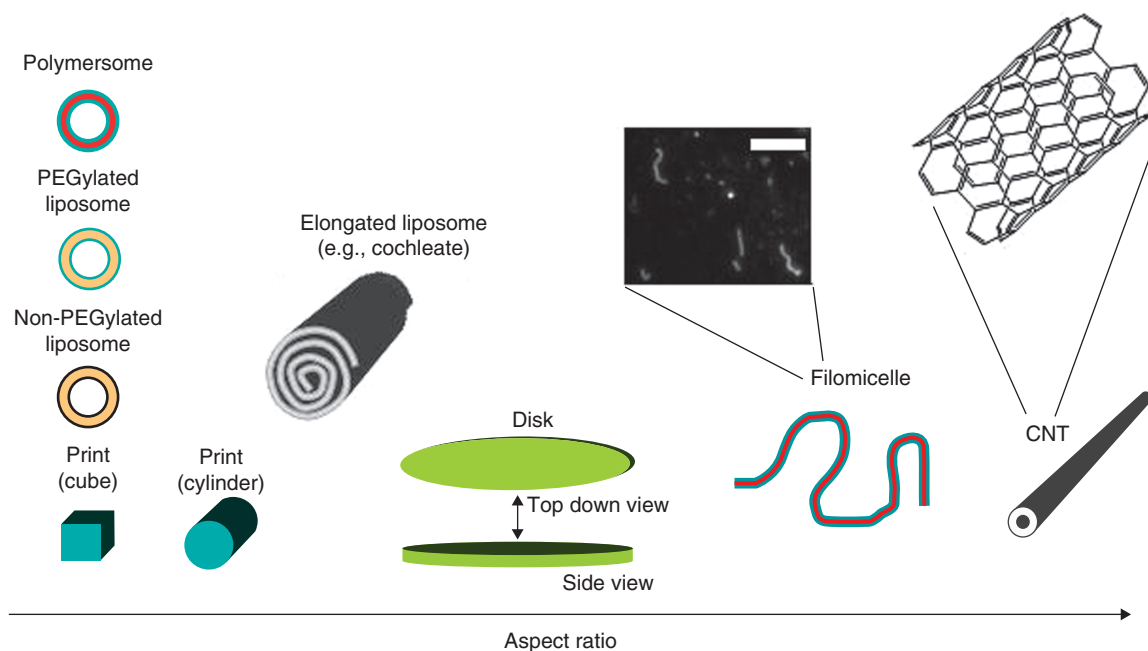


**Figure 1. DDS geometries.** Schematics of the different geometry carriers are shown in order of increasing aspect ratio. It should be noted that PRINT particles are crosslinked PEG nanogels, as opposed to the other PEGylated drug delivery systems (DDS) where one end of the PEG is free. Blue indicates PEGylation. Red indicates hydrophobic polymer. Thick black lines on liposomes represent polar groups of phospholipids, while yellow indicates non-polar tails. A blown-up fluorescence microscopy image of PEO – PCL filomicelle is shown, where the carrier was stained with the lipophilic dye PKH26. Scale bar is 10 µm. Filomicelles were formed with standard film casting/dehydration and subsequent rehydration with polymer purchased from Polymer Source Inc., Dorval (Montreal), Quebec, Canada. The common chemical structure is shown in the blown-up image of CNT. Structure is 5,5-armchair conformation for a non-spiraled SWNT.

to form solid micron-scale polymer shapes [24]. A different nanofabrication technique, nanoimprinting, afforded formulation of non-spherical nanoparticles loaded with different drugs in a relatively high-throughput manner [25,26]. This formulation, referred to as PRINT, or Particle Replication In Non-wetting Templates, provides submicron cubic, trapezoidal, conic, bar (rectangular prism) and cylindrical geometries, to name but a few. The distinguishing feature of this formulation from other imprinting techniques is the utilization of a non-wetting substrate, typically a fluorinated material. Through the use of this non-wetting substrate in addition to a non-wetting mold, the stamped material between the substrate and the mold does not stick to either component. Furthermore, there is no 'scum layer' connecting the printed particles on the substrate side, a typical problem with traditional nanoimprinting techniques. One drug delivery-friendly material utilized for these particles is a PEG-based nanogel.

## 2.5 Flexible filamentous nanocarriers

Filamentous polymeric structures represent another class of anisotropic drug delivery nanocarriers. Inspired by the self-assembly of amphiphilic phospholipids, these polymeric analogs of liposomes typically consist of diblock co-polymers of hydrophilic PEG and a hydrophobic moiety such as poly(caprolactone) (PCL), poly(lactic acid) (PLA), poly(ethyl

ethylene) (PEE) or poly(butadiene) (PBD) (indicated as OCL, OLA, OEE and OBD, respectively) and nearly monodisperse in molecular weight (MW) when produced by anionic polymerization. Two other commonly utilized options are hydrophilic poly(acrylic acid) and hydrophobic polystyrene. These diblock co-polymers are of modest size (MW typically < 50 kD) and > 20% of the mass arises from the hydrophobic block. Formulation methods are similar to those used for liposomes, for example film casting/dehydration followed by rehydration with water and heat. They self-assemble into a series of polymer micelle structures, dependent on the diblock chemistry: polymersomes (spheres with diameters from ~ 50 nm to several µm [2]) and filomicelles [27] (width ~ 10 – 40 nm, length up to 50 µm [28]). Through control of the ratio of the hydrophilic PEG (or PEO) block to the hydrophobic (e.g., PEE) block, diblock copolymers form either polymersomes, with PEG fractions of ~ 25 – 40% of each polymer molecule [29] or filomicelles, with PEG fractions of ~ 42 – 50% [27] in solvent-free solutions. Spherical micelles are the dominant species formed at PEG fractions > 50% [27].

The key distinction between *polymersomes* and spherical micelles is that the former have an interior aqueous cavity, which is absent in the latter. The diameter of filomicelles [30] and the thicknesses of polymersome membranes [31] are

larger than the membranes of liposomes: hydrophobic core thicknesses are  $\sim 40$  nm (note:  $d_{\text{lipid}} = 3 - 4$  nm). Increased  $d$  endows filomicelles and polymersomes with structural stability that persists for months for PEE-based polymersomes and can be tuned to days or hours by blending of less stable blocks (e.g., PCL) into filomicelles [32].

The filomicelles are semiflexible filaments, stiff enough to be elongated and flexible enough to bend in response to thermal fluctuations in solution (Brownian motion). The persistence length  $l_p$ , essentially the length-normalized end to end distance of a filomicelle in solution, describes its stiffness. Microscopy under static and flow conditions showed that  $l_p$  of filomicelles typically varies from 0.5 to 5  $\mu\text{m}$ , depending on the MW of the co-polymer [30]. At 37°C in aqueous media, the relaxation time of the polymer, that is the time that it takes the polymer to spontaneously randomize its conformations, is on the order of seconds, which explains the ability of filomicelles to adjust to flow [33], important from the standpoint of their behavior in the body.

In another formulation, the antioxidant enzyme, catalase, was encapsulated in its active form within nanofilaments of comparable geometry (width  $\sim 50$  nm, length 5 – 20  $\mu\text{m}$  [34]). Composed of the biocompatible PEG – PLA diblock copolymer, these carriers were formulated with a freeze – thaw solvent evaporation emulsion. It is of note that control of the polymer composition dictated whether spherical or filamentous carriers are produced in this formulation. While the absolute ratios of hydrophobic to hydrophilic blocks in the polymer were slightly different than those utilized to form polymersomes or filomicelles, the trend was the same, that is intermediate PEG contents yielded filamentous carriers, whereas higher PEG contents resulted in spherical polymer nanocarriers. The versatile drug loading features of filamentous carriers and their pharmacokinetic profile endow this geometry with unique potential for drug delivery.

## 2.6 Carbon nanotubes

High aspect ratio carbon nanotubes (CNT) composed of carbon graphene sheets represent yet another prospective non-spherical drug delivery platform. CNT are typically comprised of either single sheets (single-walled nanotubes, SWNT) or multiple concentric sheets (multi-walled nanotubes, MWNT). CNT are characterized by an enormous surface area to volume ratio (diameters as small as a few nanometers and lengths up to a few centimeters [35]), offering great potential for drug loading (see Section 3). CNT are typically stiff, with a Young's modulus (proportional to the flexural modulus) roughly 1000 times higher than that of a microtubule ( $> 1$  TPa vs 2 GPa, respectively) [36]. This results in a structure that lacks the longitudinal flexibility of filomicelles at temperatures above their glass transition temperature (typically below room temperature). A more thorough review is given on CNT and other carbon nanostructures such as nanohorns (sub-100 nm spherical aggregates of SWNT) [37].

Most CNT DDS are being studied *in vitro*. Concerns regarding CNT utility as a DDS arise from their resemblance to carcinogenic asbestos fibers and potentially long *in vivo* persistence times due to a lack of hydrolysable bonds. Rigorous animal studies are required to determine the risk/benefit ratio of CNT DDS. One can imagine the ideal combination of a CNT DDS that undergoes catch-and-release at the intended site of delivery, long enough for dumping of its drug cargo payload, yet is capable of rapid excretion once this mission is accomplished. Another option would be to incorporate degradability into CNT. Thus, despite concerns of the safety of CNT as a DDS, there are potential solutions that may reduce side effects.

## 3. Drug loading, stability and release

### 3.1 Drug loading

Drug-loading capacity is a key feature of potential DDS. Among elongated liposomes, loading hydrophobic drugs into the lipophilic membrane or hydrophilic drugs into the aqueous interior follows general approaches developed for their classic spherical counterparts. Cochleate particles provide solid hydrophobic carriers, ideal for loading of either hydrophobic, amphiphilic, or charged drugs [38]. Amphotericin B lipid complex (ABLC<sup>TM</sup>), or Abelcet, ribbon liposomes have already been utilized for treatment of AIDS-related cryptococcal meningitis and other fungal infections [39]. Interestingly, intercalation of amphotericin B within the ribbon liposomes reduced its side effects.

Polystyrene carriers including spheres and flat disks are less amenable to drug loading into the carrier. However, incorporation of fluorescent dyes into the polymer material provides a useful model carrier for tracing localization in the body and cells. Since polystyrene particles are not biodegradable, they are not commonly considered as drug carriers for medical use. However, some drugs such as therapeutic polypeptides can be immobilized on the carrier surface through hydrophobic interactions and are used for testing local effects of targeted therapeutics in animal models [11]. This method may be useful for delivery of enzymes, particularly when the ultimate goal is simply dumping of the drug payload at the site of therapy.

PRINT nanocarriers provide a versatile platform for drug loading during their formulation. For example, doxorubicin loaded into cubic PRINT nanoparticles made of crosslinked, PEG-based polymers demonstrated significant cytotoxicity with HeLa cells [40]. A disulfide bond-containing crosslinker was also incorporated that enabled the release of doxorubicin in reducing environments. PRINT nanoparticles composed of proteins such as albumin have also been formulated, some encapsulating siRNA and Abraxane (albumin-bound paclitaxel) [41].

Diverse drugs can be loaded into spherical and filamentous polymersomes and filomicelles. Hydrophobic and amphiphilic drugs [42] can be intercalated into the hydrophobic polymer membrane of polymersomes and filomicelles. Less hydrophobic



compounds including targeting moieties can potentially be coupled to the surface of polymersomes and filomicelles [43], or encapsulated within the inner aqueous cavity of polymersomes. Loading of hydrophobic drugs into filomicelles is more effective than into spherical micelles, likely due to the enhanced potential volume available for loading, based on simple geometric calculations of relative volume to surface area ratios [44]. Cancer chemotherapeutics have been the primary model drug category tested in these carriers. Loading of the hydrophobic drugs paclitaxel and doxorubicin into polymersomes and filomicelles reduces their systemic toxicity and enhances antitumor effects in animal models [32,44,45].

It is also possible to emulsify drugs into spherical particles (e.g., PLGA w/o/w emulsion particles) before stretching into elongated disks by the same methods used to make polystyrene disks [22]. This technique depends greatly on the susceptibility of the drug to inactivation upon heating and the degree of necessary heating of the original particle. This is a function of the material's glass transition temperature, the target temperature for particle stretching. For PLGA, the glass transition temperature is typically on the order of 50°C. The potent yet labile antioxidant enzyme, catalase (a tetrameric protein with MW ~ 250 kDa) was encapsulated without inactivation in a DDS composed of PEG – PLA with diverse geometries, including spherical and filamentous DDS [34]. These were formulated with a freeze – thaw modified double emulsion, enabling encapsulation of *active* enzyme. This formulation method was first tested with loading of the same enzyme but into 300 – 400 nm spherical PEG – PLGA/PLA particles [8]. Not only was active catalase encapsulated within these PEG – PLA filaments and spheres, but this therapeutic enzyme was protected from inactivation by external proteases. This is not yet realized with the typical processing utilized to form filomicelles, which can involve denaturing heating steps. On a side note, another approach even formulated filaments from peptides, subsequently loaded with doxorubicin [46]. More specifics of these peptide-carriers are covered in section 5 on targeting, the primary goal of this particular study.

The drug loading capacity of CNT is a complex subject. Drugs are typically either linked to the CNT surface, or loaded in the interior. The true interior loading capacity of CNT, which is thought to be very dependent on the interior radius, deserves a more systematic study. First, there is a volume constraint, that is maximal loading restricted by small radii typically encountered. The internal loading volume is proportional to the radius squared, thus exacerbating this volume limitation. More importantly, loading into CNT is dependent on factors such as capillary action, drawing a drug inside of what is essentially a pipe with an inner diameter of only a few nanometers. In the case of cisplatin (an anticancer drug) loading, the minimum diameter necessary to load the drug is 0.48 nm, and the optimum loading (or maximum suction energy) occurs when the diameter is only slightly larger, ~ 0.53 nm, based upon

energetic arguments and modeling [47]. The loading capacity appears to be slightly different for titania nanotubes (~ 400 nm long with inner diameters approximately 70 – 80 nm) that represent an alternative to CNT. Loading of the model protein cargoes albumin and lysozyme into titania nanotubes was performed with ~ 50 – 90% efficiency [48]. It is tempting to speculate that such highly effective loading of proteins, especially therapeutic enzymes, may be achieved without their inactivation, a concept worth direct experimental testing.

### 3.2 Degradation properties, stability and drug release

Biodegradability is one of the key requirements for biocompatibility of a DDS if its size does not permit excretion via physiological pathways including renal filtration, hepatic production of bile or exhalation from the lungs. Some nanocarriers appear to be able to safely employ these routes. Further, it appears that some cell types tolerate intracellular residence of inert polymer particles, a paradigm that can endow some 'non-degradable' nanocarriers with medical utility. For example, cell culture and animal studies suggest that non-biodegradable polystyrene nanoparticles taken up by vascular endothelial cells do not cause detectable damage in mouse organs after administration [49]. More rigorous studies are needed in this area, in the context of known toxic effects of micron and nanometer range particles in the cardiovascular and nervous systems.

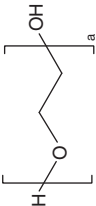
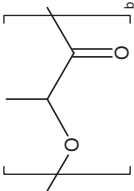
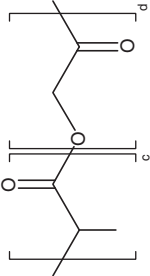
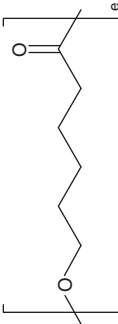
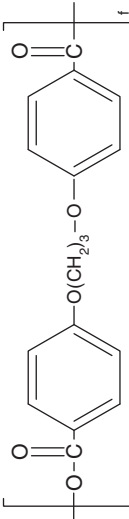
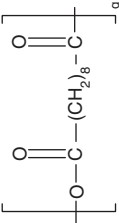
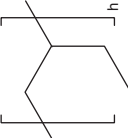
On a cautionary note, a few studies of CNT in animal models have revealed significant side effects, potentially due to the non-degradable nature of these carriers. For example, intraperitoneal administration of stiff MWNT (~ 10 µm in length) induced mesothelioma in mice [50]. In this situation, carcinogenesis is thought to be the result of inflammation that ensues from extended residence of non-digestible/degradable objects [51]. These persistent materials may cause subsequent accumulation of inflammation-associated reactive oxygen and nitrogen species. One potential solution may involve utilization of less immunogenic materials. For instance, as an alternative to CNT, titania nanotubes have been developed. Titania nanotubes are oxide coated titanium nanotubes that, by virtue of this coating, may have enhanced biocompatibility [48].

However, to be widely applicable in medicine, DDS should be biodegradable and their degradation products non-toxic, amenable to physiological excretion. Phospholipid liposomes represent a classical example of fully degradable DDS. Among biodegradable polymeric DDS materials, there are two classic examples at opposite ends of the degradation kinetics spectrum. On the fast end are polyanhydrides. On the slow end are polyesters (used for synthesis of many nanocarriers), with degradation times ranging from weeks to years, dependent on their environment and geometry [52-54]. These and other common DDS polymers are described in Table 1.

#### 3.2.1 Polyanhydrides

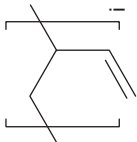
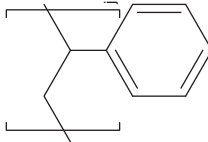
A classic example of rapidly degrading materials is polyanhydrides, typically used for formulation of microspheres. These particles have tunable degradation times from hours

Table 1. Common drug delivery system polymers.

Polymer	Structure	Degradation times	Primary degradation products
Polyethylene (glycol/oxide) PEG (aka PEO, POE)		Non-degradable	–
Poly(lactic acid) PLA		Weeks – months	Lactic acid
Poly(lactic-co-glycolic acid) PLGA		Weeks – months	Lactic and glycolic acid
Poly(caprolactone) PCL		Months – years (500+ nm spheres) Days (≤ 50 nm Ø filaments)	6-hydroxycaproic acid
Poly(carboxy-phenoxy propane) P(CPP)		Months (alone) hours – days (w/SA)	CPP (carboxylic acid)
Poly(sebacic acid) P(SA)		Minutes (alone) Hours – days (w/CPP)	SA (carboxylic acid)
Poly(ethyl ethylene) PEE		Non-degradable	–

Details of several polymers commonly used for synthesis of non-spherical carriers are shown. For those that are degradable, degradation time scales and products are also indicated.

Table 1. Common drug delivery system polymers (continued).

Polymer	Structure	Degradation times	Primary degradation products
Poly(butadiene) PBD		Non-degradable	-
Polystyrene		Non-degradable	-

Details of several polymers commonly used for synthesis of non-spherical carriers are shown. For those that are degradable, degradation time scales and products are also indicated.

to weeks, achievable by alteration of the ratio of constituent co-polymers [55-57]. Examples of these copolymers are poly(carboxy-phenoxy propane) (CPP, relatively hydrophobic) and poly(sebacic acid) (SA, relatively hydrophilic). Higher CPP:SA ratios result in slower degradation and vice versa. Similarly, blending in random PEG blocks into the poly-anhydride backbone enhances polymer hydrophilicity and thus degradation [58]. Polyanhydride carriers have been synthesized on the nanoscale [59-61], yet careful control of morphology of such DDS has not been documented. Typically there is a high poly dispersity index (PDI), or significant spread in MW distribution of the bulk poly-anhydride material, whereas near monodisperse polymer MWs are necessary for synthesis of homogenous, size-controlled non-spherical carriers.

### 3.2.2 Polyesters

From a diffusion standpoint, geometry has a profound impact on degradation of carriers based on relatively slow degrading polymers, such as polyesters. Kinetics of water penetration into, and therefore degradation of, a polymer matrix is inversely proportional to the minimum dimension of a carrier, that is the radius for a sphere. Polyester spheres on the millimeter scale exhibit surface erosion in aqueous environments; the surface degrades and the degradation products erode away from the structure faster than water can penetrate into and degrade the sphere's interior. In contrast, nanometer scale polyester spheres experience uniform water penetration throughout the polymer matrix leading to homogeneous degradation and erosion, or uniform degradation throughout the matrix. The internal degradation can actually exceed exterior degradation as acidic degradation products accumulate inside the carrier, further decreasing the interior pH.

Innate properties of the polymer backbone also regulate water accessibility to scission of individual polymer chains within a carrier: Figure 2. For instance, PCL has longer alkane segments between hydrolysable bonds than PLA or PLGA. Longer alkane segments that are free of functional groups mediate tighter polymer chain packing, enhancing crystallinity and decreasing water penetration into macromolecular structures of these polymers. Similarly, polymers composed of the same-handed enantiomer tend to pack tighter, are more crystalline and thus more resilient to degradation than polymers composed of racemic mixtures of both handed enantiomers. For example, D-PLA degrades much slower than D,L-PLA [62,63]. Likewise PLGA, which consists of random glycolic acid segments inserted into the backbone of PLA polymer chains, are even less crystalline and more susceptible to degradation. Glycolic acid is also devoid of the side methyl groups found in lactic acid, further enhancing water accessibility to PLGA chains. It should be noted that the degradation products of these typical DDS polymers are thus primarily lactic acid and/or glycolic acid monomers. These low MW (< 100 Da) monomers, physiologically produced in the body (e.g., lactic acid is

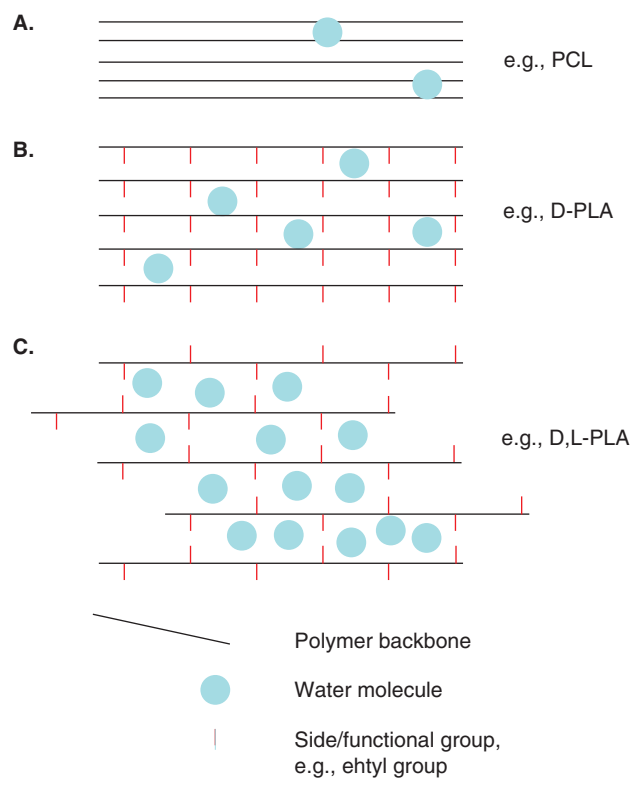


**Figure 2. Degradation and crystallinity.** **A.** Crystallinity is enhanced by tighter packing of polymer chains, depicted as black bars. Higher crystallinity reduces water penetration, depicted as blue circles, and thus slows down hydrolytic polymer degradation. **B.** Introduction of sidegroups with a uniformly chiral carbon backbone (shorter, red bars), such as methyl or ethyl groups, increase the minimum space between packed polymer chains, thus further enhancing water penetration and polymer degradation. **C.** This reduced efficiency in polymer chain packing is exacerbated when randomly two-handed polymers, that is a racemic mixture, are combined into a structure, yet again enhancing water penetration/degradation.

produced in hypoxia) and found in food, are very hydrophilic, diffusible and rapidly metabolized, therefore posing little threat of toxicity in living systems (although excessive local build-up of lactic acid and acidification may lead to pathological consequences; accumulation of lactate in hypoxic tissues is one of the reasons for hypoxic pain).

### 3.2.3 Geometric and environmental parameters of carrier degradation

A new and interesting paradigm ensues when one considers non-spherical geometries, namely nanofilaments. In general, self-assembled micelles such as polymersomes and filomicelles composed of OLA and OCL degrade by PLA and PCL hydrolysis [53,54] into smaller non-toxic monomers and oligomers cleared by renal and hepatic excretion [64]. OCL hydrolysis yields pore-preferring copolymers [32] and filomicelle fragmentation [65]. The degradation can be delayed by blending OCL or OLA with stable, non-degradable

diblocks (e.g., PEG – PEE < 40 kD, that are excreted by kidneys). Interestingly, it was found that PEO – PCL filomicelles exhibit rapid degradation kinetics on the order of days, despite the fact that PCL is typically thought of as a slow-degrading material with kinetics on the order of months to years [65]. This result was verified by fluorescence and transmission electron microscopy, and gel permeation chromatography measurements of released degradation products. It appears that due to the relatively small distances that water would have to diffuse across with filomicelles (cross-sectional radii of only 5 – 15 nm) it is possible for PCL to undergo relatively rapid degradation. It should be noted that by simply increasing the OCL MW by slightly more than twofold, the filomicelles' diameter nearly tripled and the degradation half-life increased over tenfold. Interestingly, since PEO does not degrade in water, the degradation occurs at the PCL end, which results in an increased ratio of PEO:PCL MWs and thus a transition to a micelle preferring polymer. Filamentous carriers composed of PEO – PLA, loaded with a therapeutic enzyme, experienced similar degradation characteristics, although the overall kinetics were longer than in classical filomicelles described above, that is on the order of weeks versus days, most likely due to a 2 – 3-fold enhancement in cross-sectional diameter (and perhaps the different formulation method) [34]. However, in both cases filamentous carriers transformed into spherical vesicles prior to complete disintegration.

In addition to geometry, environmental factors including acidity and the presence of destructive hydrolytic enzymes play a key role in degradation. Degradable polymers typically contain hydrolysable bonds and undergo faster acid-catalyzed hydrolysis at low pH [66]. For example, the rate of polymersome hydrolysis and release of loaded drugs is further accelerated at acidic lysosomal pH (~ 5.0) [45]. The enzyme-loaded PEO – PLA nanofilament preparation mentioned earlier also demonstrated significant pH-dependent degradation, wherein lower pH accelerated transformation of the filaments into vesicles before complete disintegration [34]. Interestingly, polyanhydrides degrade more slowly in acidic pH conditions, with far more rapid degradation rates occurring in basic solutions [60,67]. Furthermore, the ester bonds in polyesters such as PLA or PCL are susceptible to degradation by hydrolases, esterases and proteases. Enzymatic degradation of biodegradable polymers, such as PLA, has been extensively studied [68-70].

Design of biodegradable DDS and mechanisms controlling their degradation represent an enormous field of research. Chemical and supramolecular carrier structures represent key parameters, modulated by environmental factors and the chemical nature of the cargo. To find the optimum balance, blending of materials with different degradation kinetics is often pursued [32,61]. However, as we have seen in this section, carrier geometry is also an important factor for modulation of degradation rate and, in some cases, even alteration of the mechanism of degradation of carriers based



on the same polymer. For example, it would seem that switching to different morphology carriers such as filaments may offer similar degradation control, reinstating the therapeutic potential of materials originally thought of as 'too slowly degrading'.

#### 4. Circulation

In order to enhance circulation properties of carriers in the bloodstream, the typical course of action is to coat a carrier with PEG. For example, PEGylation of liposomes increased their half-life from less than 30 min to approximately five hours in mice [71]. Other benefits, such as reduced interaction with the immune system, have also been found. For example, due to their dense PEG surface brush, polymersomes and filomicelles are compatible with blood [2,31,72], as they: i) remain suspended and flexible in plasma; ii) do not adhere to red blood cells and leukocytes in blood; iii) do not fix opsonins or activate complement [2,31]; and iv) do not cause hemolysis [30].

Besides surface chemistry, geometry and physical properties of the DDS regulate its circulation *in vivo*. Most extensively studied has been the effect of the size of spherical carriers on their half-life in the circulation. Particles over 100 nm are typically retained mechanically by the spleen [73]. Small spherical structures (< 20 nm) permeate through all fenestrated endothelia (e.g., in kidneys, liver, spleen), resulting in an increased rate of clearance from the circulation. For large spherical structures (e.g., > 1  $\mu\text{m}$ ) clearance rates are also high for multiple reasons. Large structures possess an increased tendency to aggregate in and be retained, mechanically, by capillaries. From a hydrodynamic standpoint, as the size increases, momentum forces begin to dominate and wall collisions become more common, resulting in an increased rate of clearance by cellular uptake. However, when spherical structures reside within the 'sweet spot' (20 nm < d < 1  $\mu\text{m}$ ), all of these clearance mechanisms are minimized and circulation times are enhanced: **Figure 3A**.

Recent work has suggested that geometry, beyond spherical diameters, may have profound effects on carrier behavior in the blood by further enhancing the capacity of the DDS to evade the body's clearance mechanisms [33]. The tendency of a carrier to resist flow or be carried along the streamlines is dictated by the balance of drag forces (viscous) and momentum forces of the carrier in the flow conditions encountered in the systemic circulation: **Figure 3B**. The density of the nanocarrier will dominate the momentum force it possesses. However, the drag forces will be determined by both the geometry of the carrier and the nanocarrier surface roughness (friction factor). Surface functionalization can have a profound impact on this friction factor. A typical example of functionalization would include PEGylation of carriers or even proteins, resulting in the extended circulation of both entities, discussed above in terms of masking carriers from clearance systems in the body [71]. In another example, clearance mechanisms of

CNT are significantly changed by relatively minor modifications to the carrier's exterior. The clearance times are generally rather short for CNT, often on the order of a few hours [74]. PEGylation may offer some enhancement in circulation time, where a small fraction of injected PEGylated CNT has remained in circulation for near one day [75]. However, in this particular study the half-life was still around an hour. In another study that utilized i.v. administration of CNT in mice, it was found that CNT surface-functionalized with autologous serum proteins accumulated primarily in the lung and liver, while CNT heavily functionalized with ammonium or carboxylate groups were primarily excreted in urine [76]. A controlled rate of elimination may attenuate toxicity and potential carcinogenicity by reducing residence time *in vivo*.

PEGylation prolonged circulation half-life of 200 nm spherical liposomes from ~ 30 min to near five hours in mice [71]. Spherical polymersomes persist in the circulation slightly longer with half-lives of near one day [33]. This is thought to be due to the much denser PEG brush present on the surface of polymersomes relative to liposomes (and, perhaps, due to their thicker bilayer and resultant structural integrity). By their design, polymersomes are made of individual polymers that possess a 100 mol% degree of PEGylation, whereas liposomes with more than 10% PEGylation of their constituent phospholipids are unstable and dissolute [77]. Interestingly, 100 nm diameter PEG-based PRINT particles appear to have minimal cytotoxicity in cell culture, yet exhibit pharmacokinetics similar to non-PEGylated liposomes in circulation, that is relatively fast blood clearance (half-life less than 10 min) and uptake primarily in the liver and spleen in mice [25]. It is of note that these were cubic particles, and the nature of their coating, crosslinked PEG (as opposed to freely flexible PEG with only one immobilized terminus, as in the case of polymersomes), may have limited their circulation potential. Therefore, both differences in geometry and chemistry could be involved in the distinct circulation profile of PEG-based PRINT carriers relative to polymersomes.

However, even in the hypothetical situation where carriers with identical chemistry (e.g., equal degrees of surface coating/modification), variations in geometry are likely to impact behavior *in vivo* significantly, particularly in the circulation. Thus, comparison of polymersomes and filomicelles based on the same polymer chemistry provides unique insight into the role of carrier geometry in circulation, **Figure 3B**. The current maximum in terms of circulation appears to be highly flexible filomicelles, with half-lives of around a week [33]. Surprisingly, even stiffer filomicelles traced by fluorescence remained in circulation for several days. This is thought to be due primarily to filomicelles' ability to align with blood flow and avoid vascular collisions, filtration and phagocytosis. It was shown that within the 1 – 20 micron length scale, longer filomicelles circulate for longer periods of time and that they are less readily internalized by macrophages, particularly in flow conditions. This is attributable

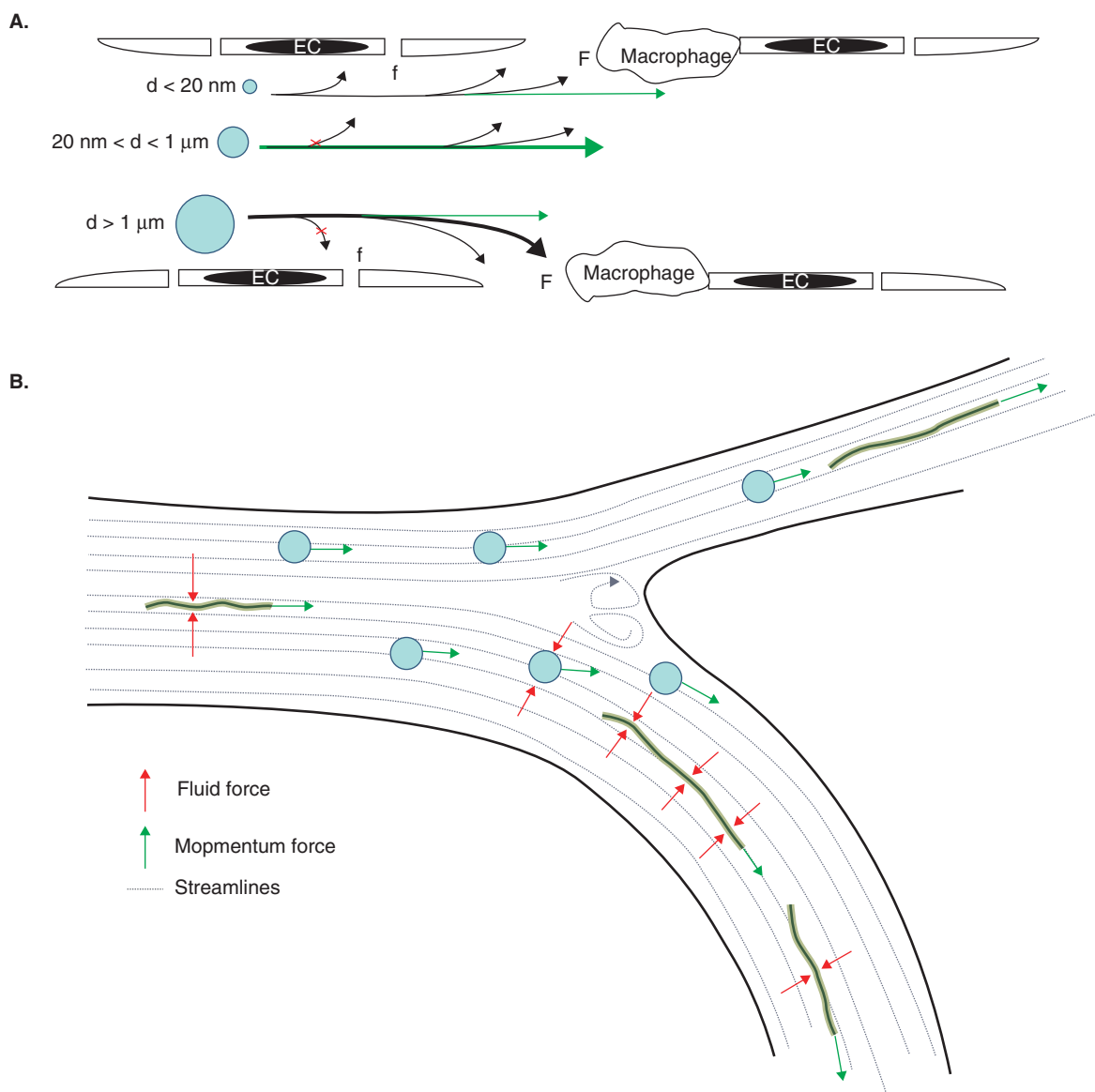


**Figure 3. Size and shape effects on circulation.** **A.** Size of the spherical drug delivery system determines the mechanism and rate of clearance. Structures which are smaller than 20nm readily pass through the fenestrated endothelium of the kidney, liver and spleen, resulting in a relatively rapid rate of clearance from the circulation. When the spherical particle diameter increases to  $> 1 \mu\text{m}$ , momentum effects begin to dominate and collision with macrophages become common, resulting in increased clearance. However, when the size falls between these two extremes, circulation times are greatly enhanced due the avoidance of these size-dependant clearance mechanisms. **B.** Effect of aspect ratio on circulation. A particle moving in along with a fluid has an internal momentum force and is being acted upon by the surrounding fluid forces. When a directional change in the vessel occurs, the fluid force acts upon the carried particle to change its direction. If the particle's momentum force exceeds the capability of the fluid force to change direction, it will collide with the vascular wall. Wall collisions increase the likelihood of interactions with the macrophages, thereby increasing the clearance rate. Flexible, elongated structures, like filomicelles, have an increased sensitivity to fluid forces, due to the aerodynamic properties brought upon by their shape. This results in structures whose momentum can be easily changed to match that of the fluid and thereby reduce the number of wall collisions.

EC: Endothelial cell; f: Small intra-endothelial fenestrae ( $< 200 \text{ nm}$  diameter); F: Large inter-endothelial fenestrae (1-5 micron) in the reticuloendothelial system.

to their extensive length in that they provide a difficult substrate for macrophages to engulf and further, that the carrier's flow-aligning body experiences extensive drag forces from directional flow. These drag forces are in opposition to phagocytosis, thus providing significant competition to cell-enveloping mechanisms. Filomicelles' internalization was observed under *static* conditions with cultured epithelial cells, thus suggesting that flow conditions are the primary barrier to phagocytosis.

Another interesting case of pure geometry effect on circulation in the bloodstream was observed in a comparison of non-PEGylated anisotropic carriers, polystyrene disks and spheres. While the circulation half-life was nowhere near as prolonged as in the case of filomicelles, protein (IgG)-coated disks (dimensions  $3 \times 1 \times 0.1 \mu\text{m}$ ) persisted in the circulation markedly longer than polystyrene spheres  $\geq$  one micron [11]. In fact, disk-shaped carriers remained in circulation for comparable times to 100 nm polystyrene spheres, despite having one dimension  $\sim 3 \mu\text{m}$ . It is quite possible that these *nanodisks* also align with flow, similar to filomicelles (or, perhaps, even more similar to discoid erythrocytes), and therefore circulate in the mainstream, avoiding vascular collisions, uptake into the reticulo-endothelial system (RES) and stacking in capillaries. Although the concept of flow alignment and non-spherical DDS with extended clearance times is relatively new, it apparently has many potential applications for prolonged circulation of DDS. Some common circulation half-lives are listed in Table 2.

## 5. Targeting

In theory, the use of non-spherical carriers may provide unique benefits for drug targeting. First, an enormous surface area to volume ratio in nano devices is further exaggerated in non-spherical carriers, which translates into a potentially large available surface area for conjugation of targeting moieties, while avoiding many of the limitations (such as capillary retention) of larger, micron-plus spheroids. Similarly, the smaller *nano* dimension of non-spherical nanocarriers allows effective perfusion via capillaries, enhancing access to diverse targets that are unreachable by micron-scale spheres. This translates into enhanced therapeutic potential, particularly in areas of increased leakiness, such as tumors and inflamed tissues.

The research on *targeted* non-spherical nanocarriers is relatively recent and limited but there are a few studies suggesting the feasibility of such DDS. Flexible filomicelles for vascular drug delivery were biotinylated via the free terminal group of PEO on a PEE – PEO diblock, before formulating this polymer into avidin-specific filomicelles [43]. The biotinylated polymer was blended in with non-modified PEE – PEO to make targetable filomicelles that could anchor any avidin-functionalized entity, such as an antibody. Biotinylated filomicelles (*b*-filomicelles) were stable, bound specifically to avidin-coated surfaces and retained their structural

integrity while bound. Furthermore, in a simplified binding study, it was shown that *b*-filomicelles can even bind the native biotin-receptors of smooth muscle cells [43]. The balance of the targetability and the enhanced circulation behavior of such flexible filomicelles is likely to be a complex interplay of cellular interaction and strength of active target binding. Further work is required to determine exactly what role long circulating worm-like structures will play in active targeting drug delivery systems..

Utilizing a different approach to synthesis of filamentous nanocarriers, another group made amphiphiles that contained hydrophobic aliphatic chains linked with a cancer targeting peptide via a high MW PEG linker [46]. They also synthesized similar molecules composed of the same aliphatic chain that contained a chelating agent in place of PEG, which was used to incorporate indium-111 for gamma camera imaging. Combining these two molecules, they were able to construct filaments with cross-sectional radii on the order of 4 nm and lengths over 70 nm. Not only did these targeted carriers demonstrate significant binding to tumor tissue *in vivo*, but they were able to load doxorubicin into these aggregates and selectively kill tumor cells *in vitro*. These initial results are promising and provide a basis for comparison of this DDS with spherical analogs.

SWNT have also been functionalized with targeting antibodies, and underwent cytoplasmic delivery in a cell culture model [78]. The relatively small CNT ( $176 \pm 77 \text{ nm}$ ) were conjugated with CD3 $\epsilon$  and CD28 antibodies, targeted to T-cell receptors, via a PEG linker. A fusogenic polymer was also included, in order to enable lysosomal rupture and cytoplasmic delivery. Another study conjugated CNT with radionuclides, while targeted to tumor cells via attached Rituximab (CD20 targeted) and Lintuzumab (CD33 targeted) antibodies [79]. The radiometal – ion chelate DOTA was conjugated to incorporate indium-111. Binding was confirmed by flow cytometry with CD20 $^{+}$ /CD33 $^{-}$  Daudi cells and CD33 $^{+}$ /CD20 $^{-}$  HL60 cells. This result was further verified with tumor-injected SCID mice.

In a murine model, polystyrene disks were coated with antibodies targeted to the pulmonary endothelium [11]. The disks,  $1 \times 3$  microns (minor and major axes, respectively) and only 100 nm thick, demonstrated remarkable targeting to endothelium and accumulation in pulmonary vessels. Interestingly, the immunospecificity index, or ratio of targeted to non-targeted carriers in a tissue or organ, was more than three times greater for disks than even the best spherical preparation (100 nm polystyrene particles in this particular study). In fact, both the specificity and efficacy of pulmonary targeting of the disks were higher than that of their spherical counterparts. This likely reflects both the superior circulation features of disks, discussed in the previous section, and the higher affinity of anchoring on the target cells. The latter advantage may come from the preferable shape of the contact surface (i.e., large numbers of antibodies immobilized on the flat disk surface can multivalently engage numerous copies

**Table 2. Clearance times.**

Nano carrier systems	CircT <sub>1/2</sub>
PEGylated liposomes	~ 5 – 15 h
Non-PEGylated liposomes	< 1 h
Polymersomes (ps)	≤ 30 h
Polystyrene flattened disks (0.1 × 1 × 3 μm)*	< 1 h
Polystyrene 100 nm spheres*	< 1 h
Micro/nanofabricated (PRINT)	< 1 h
Filomicelle	≤ 1 wk
Carbon nanotube (CNT)	≤ 3 h

\*Carriers that were coated with non-specific control protein IgG prior to injection. The circulation half-lives of different geometry carriers are displayed. Pharmacokinetics were determined via intravascular injection in mice.

of cellular antigens) and the hydrodynamic features (that is drag force detaching an initially adhered carrier from the cell surface is much less in the case of thin flat disks compared to spheroids).

## 6. Cellular uptake and subcellular trafficking

Vesicular uptake by phagocytes (e.g., by macrophages) has been studied for more than a century in the context of immunity, that is mechanisms of elimination of pathogens and particles, antigen presentation, inflammation and cancer. An enormous body of literature informs us that the efficacy and pace of phagocytosis and subsequent lysosomal delivery and destruction of internalized materials, as well as the phagocyte's reaction (degranulation, respiratory burst, antigen presentation) depend on the size and shape of particles, among their other features (surface hydrophobicity, antigenic or sugar determinants, rate of opsonization by complement and immunoglobulins, etc). It should be noted that pathogen internalization may involve signaling and other activities of both a microbe and phagocyte. Interestingly, even inert particles may 'imitate' internalization signals of microbes, by crosslinking specific cell-surface determinants, or initiation of membrane fusion and penetration [80]. Phagocytosis of particles is a subject important in DDS design from the standpoint of elimination and side reactions caused by DDS interactions with macrophages and other components of the RES [81]. Recent literature on this subject includes systematic studies on the role of size and shape of opsonized polystyrene particles in phagocytosis, discussed below. However, a review of modulation of phagocytosis by geometry of the objects exceeds the scope of this paper.

The lysosomal destination is typical for internalized ligands, yet the kinetics of lysosomal delivery varies depending on the type of receptor, ligand size and endocytic pathway [82-85]. Macrophages internalize and deliver > 1,000 nm IgG-opsonized particles to lysosomes faster than < 500 nm particles [84].

Parenchymal cells internalize < 100 nm particles faster than > 500 nm particles [86], unless they have an elastic membrane [87]. The rate of phagocytosis of rigid elongated disks, that have no targeting ligand, is dependent on the degree of curvature of the disk at the point of contact [19]. Essentially, disks are only phagocytosed if macrophages initially contact one of the narrow ends of the carrier. If the point of contact is on a broad side of the disk (low radius of curvature), there is no effective phagocytosis. Similarly, stiff worms of the same composition are only internalized if the point of contact is at the carrier's point of maximum curvature, namely the ends [88]. This concept is illustrated in Figure 4.

Among non-phagocytic cells, the vascular endothelium arguably represents one of the most important targets for intracellular and transcellular delivery. Endothelial cells internalize ligands by phagocytosis and endocytosis via caveoli [89], clathrin-coated [90] and uncoated vesicles [4], and macropinocytosis for fluid phase uptake [91]. Antibodies to vascular cell adhesion molecule (VCAM) and selectin enter endothelial cells via constitutive clathrin endocytosis [92,93]. Selection of epitope-specific VCAM-1 ligands further activates endocytosis [93], enhancing vascular VCAM-1 imaging in animal models of inflammation [94]. Endothelial cells do not internalize monomeric antibodies to intercellular adhesion molecule (ICAM) or platelet endothelial cell adhesion molecule (PECAM) but internalize multivalent anti-ICAM and anti-PECAM conjugates [9,91] that cluster cell adhesion molecules (CAM), triggering endothelial uptake via a unique pathway, CAM-mediated endocytosis [91]. Interestingly, CAM-endocytosis of nanoparticles targeted to PECAM-1 and ICAM-1 seems to be dependent on their geometry. Thus, upon attachment of anti-CAM targeted nanocarriers, the rate of internalization by endothelial cells is markedly faster for spheres relative to disks [11]. This appears to be relatively independent of the radius of curvature at the initial point of contact, although this feature was not rigorously tested in this study. Nevertheless, fluorescence and electron microscopy showed that endothelial cells effectively internalize anti-CAM disks in cell culture and *in vivo* in pulmonary vessels without detectable cellular and pulmonary damage [11].

Furthermore, intracellular trafficking of anti-ICAM was modulated by carrier geometry. Spherical anti-CAM carriers arrive in lysosomes ~ 2 – 3 h after uptake [9,10,91]. The lysosomal lytic enzymes, reducing agents and low pH can facilitate release of drug cargo. Target CAMs co-internalized from the endothelial surface with anti-CAM carriers dissociate from the carriers in endosomes [10] due to lowering pH [95]. The carriers traffic to lysosomes, while CAM recycles to the endothelial surface, allowing multiple cycles of intracellular delivery *in vitro* and *in vivo* [10]. This provides an attractive pathway for sustained drug delivery by long-circulating carriers targeted to CAMs expressed in pathological sites, such as inflammation foci. Interestingly, disk anti-CAM carriers trafficked to lysosomes slower than their spherical

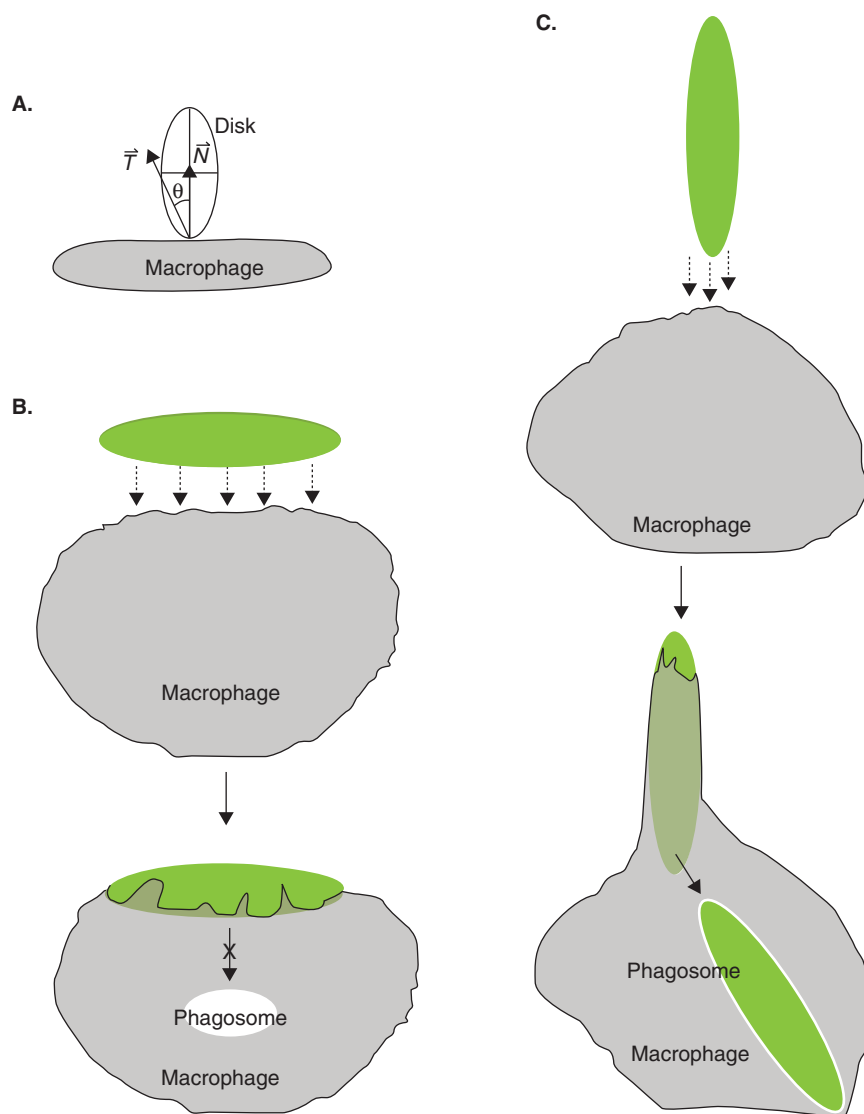


**Figure 4. Phagocytosis of anisotropic geometries.** The initial point of contact of a disk-shaped carrier (e.g.,  $0.1 \times 1 \times 3 \mu\text{m}$ ) with a macrophage determines whether or not phagocytosis/internalization occurs. **A.** The angle,  $\theta$ , between the vector normal to the surface of the cell ( $\vec{T}$ ) at the point of contact and the vector from the point of contact through the midline of the carrier ( $\vec{N}$ ) predicts whether complete phagocytosis occurs [19]. **B.** For larger  $\theta$ , phagocytosis is inhibited. **C.** However, for small  $\theta$ , internalization is possible, even when the major axis of the carrier is larger than a few microns.

counterparts; hence the former carriers were advantageous for delivery of antioxidant enzymes (which work effectively only in prelysosomal compartments), whereas the latter were ideal for delivery of lysosomal hydrolases for enzyme replacement therapy [11].

Internalization mechanisms of other non-spherical carriers have also been investigated. For instance, short SWNT ( $\sim 200 \text{ nm}$  long) coated with BSA or DNA are internalized by cancer cells (HeLa) primarily by a clathrin-coated pit pathway [96]. Another study demonstrated not only internalization, but also exocytosis of DNA-coated SWNT with similar kinetics as endocytosis [97]. This study was not as focused on

the particular intracellular mechanism observed in fibroblasts but rather on single particle tracking and characterization of kinetics of this SWNT transport phenomena. It is also conceivable that other chemical functionalizations, such as covalent modification with ammonium or methotrexate, may also enable internalization of CNT, non-specifically in multiple cell types [98]. The authors of this particular study postulated that penetration may be the result of CNT-puncturing of cell membranes. Similarly, researchers suggested that PEG-based cylindrical PRINT particles are internalized primarily via clathrin-mediated endocytosis and macropinocytosis in HeLa cells [25,26]. The cylindrical particles used were



Table 3. Nanocarrier summary.

Nano-carrier systems	Size	Typical shapes	Common materials	Ex's of loaded drugs
PEG-ylated liposomes	50 – 500 nm	Spherical	Phospholipids ( $\leq 10\%$ PEGylated)	Dox, Taxol
Elongated liposomes	$\leq 5 \mu\text{m}$ (L) $\times \sim 100 \text{ nm} - 2 \mu\text{m}$ ( $\varnothing$ )	Tubules, cochleate, or ribbon	Phospholipids	Amphotericin B
Polymersomes (ps)	50 – 5,000 nm	Spherical	PEO-b-(PEE, PBD, PCL, or PLA)	Dox, Taxol
Flattened disks	$\leq 14 \mu\text{m}$ (major axis) $\times \sim 3 \mu\text{m}$ (minor) $\times 400 - 1000 \text{ nm}$ (thick)	Flattened ellipsoid	Polystyrene, PLGA	Acid sphingomyelinase, catalase, ICAM Ab
Micro/nano of abricated (PRINT)	e.g., $200 \text{ nm } \varnothing \times 150 \text{ nm}$ tall (cylinder)	Cubic, elongated cylinder	PEG (cross linked nanogel), albumin	Dox, siRNA, Abraxane
Flexible filaments (Filomicelles)	$\leq 5 - 50 \mu\text{m}$ (L) $\times 10 - 40 \text{ nm}$ ( $\varnothing$ )	Elongated	PEO-b-(PEE, PBD, or PCL)	Taxol, PKH26
Freeze thaw double emulsion polymer nanocarriers	350 nm	Spherical	PEG-b-(PLGA or PLA) ( $\sim 60 - 78\%$ PLA or $\sim 79\%$ PLGA)	Catalase, peroxidase, xanthine oxidase
Freeze thaw double emulsion polymer nanocarriers	$5 - 10 \mu\text{m}$ (L) $\times 50 - 70 \text{ nm}$ ( $\varnothing$ )	Elongated	PEG-b-PLA ( $\sim 80 - 95\%$ PLA)	Catalase, PKH26
CNT	$\leq 5 \text{ nm } \varnothing \times \leq 5 \text{ cm}$ (length)	Elongated	Carbon graphene sheet	Cisplatin

The major drug deliver systems of varying geometry are listed, along with pertinent details such as size, materials and drugs loaded.

approximately one micron in diameter and  $\sim 680 \text{ nm}$  in height. Similar internalization results were observed in fibroblasts, ovarian carcinoma cells, breast cancer cells and macrophages. In pulmonary epithelial cells, initial results suggest that filomicelles may undergo fragmentation upon macropinocytosis, before trafficking to the perinuclear region [33]. Another factor that may come into play is the stiffness of such anisotropic carriers. Previous studies with spherical particles of varying rigidity suggest that this parameter is quite important in phagocytosis [99]. Hence, highly flexible filomicelles, or any other non-spherical carrier may also present unique advantages/disadvantages purely by virtue of their stiffness. Collectively, these results suggest that there are potentially many new/unanticipated internalization pathways and mechanisms for non-spherical DDS.

## 7. Conclusion

This review addresses the emerging field of non-spherical geometries in drug delivery. These novel carriers, summarized in Table 3, range from elongated liposomes, to stretched, flat disks, to filamentous micelles. Several desirable features are combined in these *nano* anisotropic DDS, such as a tremendous drug loading potential and enhanced pharmacokinetic profiles. Exploration of these carriers in drug targeting and sub-cellular addressing are becoming increasingly more active, and the combination of these avenues with the unique flow profiles of non-spherical carriers is no doubt at the forefront of the field.

## 8. Expert opinion

One of the more recent driving events in novel DDS morphology was the dawning of the nanotechnology era. While nanotechnology as a science is arguably as old as colloidal chemistry, its applications in terms of the design of DDS with controlled geometry has taken form more recently, in the past decade. One of the earliest findings was that *nano*-scale particles had much improved circulation behavior relative to micron-sized carriers. Further, these smaller vehicles had improved penetrating power, particularly into areas with increased permeability, such as those afflicted by inflammation or cancer. However, the vast majority of nanocarriers used at the time were spherical: carriers of this shape are energetically favorable and hence more readily produced. Only a few laboratories had investigated the potential of non-spherical carriers, such as elongated liposomes, in terms of drug delivery.

One of the first steps towards exploring anisotropic *nano*-geometries was perhaps a result of the relaxation of the definition of what is truly *nano*. If an object only has to be nanometric in one dimension, a whole new realm is possible. One only has to look as far as one's car, for example, for nanocomposite material bumpers. These can be on the meter length scale, yet contain embedded CNT-dimension fibers to impart superior strength, reduced brittleness and significantly reduced weight, among other benefits. By a similar definition, CNT and filomicelles, in particular, are also *nano*, despite the obvious fact that their maximal dimension (length) may exceed several microns.

Successful synthesis of these structures led to exploration of the role of carrier geometry in drug delivery. Like so many other areas of biotechnology, bio-inspired design reveals the true potential of nanofilaments as a DDS. Influenza, bird flu and Ebola, to name but a few, are all filamentous viruses with dimensions very comparable to filomicelles. Geometry assists the potency of these viruses in humans, and thus it is plausible that the very same geometry advantages may assist carriers with therapeutic drug cargos.

Keeping in mind what was necessary to bring the niche of non-spherical geometry drug delivery to its current place, where it will go and what steps are necessary are of equal importance. As has been witnessed with CNT and the potentially extreme deleterious effects of prolonged DDS residence, biodegradability, or at least a method for rapid clearance of long-persisting materials, should remain a key component. The same can be said of polystyrene carriers, elongated or spherical. Different coating materials have already had modest success in addressing this issue. Another approach may involve the incorporation of hydrolysable bonds, or at least a blending of degradable with non-degradable materials. A mechanism to ensure macromolecular breakdown into materials that are easily excreted, such as non-aggregated low MW polymers or monomers, might assist in the physiological tolerance of many of these DDS. This approach is quite feasible with polymersomes [32] and could provide solutions to toxicity issues with other carriers. Furthermore,

control of carrier geometry offers an additional factor in regulation of its degradation.

Stiffness, or flexibility, particularly for filamentous DDS, will become a key design parameter as this seems to have a direct effect on the pharmacokinetics of the carrier [33]. Regardless of stiffness, the non-spherical property translates into the flow alignment paradigm, which carries across all elongated, non-spherical carriers, Figure 3B. If *nano* carriers can maintain this flow alignment property, and thus avoid capillary retention or RES clearance, they may maintain the penetrating power characteristic of spherical *nano* carriers, while containing the payload typical of micron-sized DDS.

Ultimately, the development of new, or the modification of existing, formulation techniques that can accommodate degradable materials, as well as drugs of different solubilities and sensitivity to inactivation (e.g., low MW, hydrophobic taxol vs high MW, hydrophilic catalase) will be of utmost importance. These techniques must be reproducible, with very homogeneous preparations. Methods should be scalable to the industry level in terms of quantity and GMP quality. This has been realized for spherical particles but the extension of formulations for non-spherical DDS from the bench to an industrial scale has yet to be explored.

### Declaration of interest

The authors state no conflict of interest and have received no payment in the preparation of this manuscript.

### Bibliography

Papers of special note have been highlighted as either of interest (•) or of considerable interest (••) to readers.

1. Lasic DD. Product review: doxorubicin in sterically stabilized liposomes. *Nature* 1996;380(6574):561
2. Photos PJ, Bacakova L, Discher B, et al. Polymer vesicles in vivo: correlations with PEG molecular weight. *J Control Rel* 2003;90(3):323-34
3. Saad M, Garbuzenko OB, Ber E, et al. Receptor targeted polymers, dendrimers, liposomes: which nanocarrier is the most efficient for tumor-specific treatment and imaging? *J Control Rel* 2008;130(2):107-14
4. Predescu D, Palade GE. Plasmalemmal vesicles represent the large pore system of continuous microvascular endothelium. *Am J Physiol* 1993;265(2 Pt 2):H725-33
5. Vallet-Regi M, Balas F, Arcos D. Mesoporous materials for drug delivery. *Angew Chem Int Ed Engl* 2007;46(40):7548-58
6. Neumaier CE, Baio G, Ferrini S, et al. MR and iron magnetic nanoparticles. Imaging opportunities in preclinical and translational research. *Tumori* 2008;94(2):226-33
7. Misra RD. Quantum dots for tumor-targeted drug delivery and cell imaging. *Nanomedicine* 2008;3(3):271-4
8. Dziubla TD, Karim A, Muzykantov VR. Polymer nanocarriers protecting active enzyme cargo against proteolysis. *J Control Rel* 2005;102(2):427-39
9. Muro S, Cui X, Gajewski C, et al. Slow intracellular trafficking of catalase nanoparticles targeted to ICAM-1 protects endothelial cells from oxidative stress. *Am J Physiol Cell Physiol* 2003;285(5):C1339-47
10. Muro S, Gajewski C, Koval M, Muzykantov VR. ICAM-1 recycling in endothelial cells: a novel pathway for sustained intracellular delivery and prolonged effects of drugs. *Blood* 2005;105(2):650-8
11. Muro S, Garnacho C, Champion JA, et al. Control of Endothelial Targeting and Intracellular Delivery of Therapeutic Enzymes by Modulating the Size and Shape of ICAM-1-targeted Carriers. *Mol Ther* 2008. p. 1450-8
- This paper demonstrates the effect of size and shape on targeting of spherical and elongated disks surface coated with therapeutic enzymes.
12. Chambers E, Mitragotri S. Long circulating nanoparticles via adhesion on red blood cells: mechanism and extended circulation. *Exp Biol Med* (Maywood) 2007;232(7):958-66
13. Inoue K, Suzuki K, Nojima S. Morphology of lipid micelles containing lysolecithin. *J Biochem* 1977;81(4):1097-106
14. Yager P, Schoen PE. Formation of Tubules by a Polymerizable Surfactant. *Mol Crystals Liquid Crystals* 1984;106:371-81
15. Lee KC, Carlson PA, Goldstein AS, et al. Protection of a decapeptide from proteolytic cleavage by lipidation and self-assembly into high-axial-ratio microstructures: a kinetic and structural study. *Langmuir* 1999;15(17):5500-8
16. Papahadjopoulos D, Vail WJ, Jacobson K, Poste G. Cochleate lipid cylinders: formation

- by fusion of unilamellar lipid vesicles. *Biochim Biophys Acta* 1975;394(3):483-91
17. Janoff AS, Boni LT, Popescu MC, et al. Unusual lipid structures selectively reduce the toxicity of amphotericin B. *Proc Natl Acad Sci USA* 1988;85(16):6122-6
18. Hayes MA, Pysher MD, Chen K. Liposomes form nanotubules and long range networks in the presence of electric field. *J Nanosci Nanotechnol* 2007;7(7):2283-6
19. Champion JA, Mitragotri S. Role of target geometry in phagocytosis. *Proc Natl Acad Sci USA* 2006;103(13):4930-4
- **This paper is the first report of the importance of geometry in phagocytosis, looking at different geometry polystyrene disks. The role of the point of contact of elongated disks in phagocytosis is of particular importance.**
20. Champion JA, Katare YK, Mitragotri S. Making polymeric micro- and nanoparticles of complex shapes. *Proc Natl Acad Sci USA* 2007;104(29):11901-4
21. Ho CC, Keller A, Odell JA, Ottewill RH. Preparation of monodisperse ellipsoidal polystyrene particles. *Colloids Polym Sci* 1993;271(5):469-79
22. Champion JA, Katare YK, Mitragotri S. Particle shape: a new design parameter for micro- and nanoscale drug delivery carriers. *J Control Release* 2007;121(1-2):3-9
23. Xu S, Nie Z, Seo M, et al. Generation of monodisperse particles by using microfluidics: control over size, shape, and composition. *Angew Chem Int Ed Engl* 2005;44(5):724-8
24. Dendukuri D, Pregibon DC, Collins J, et al. Continuous-flow lithography for high-throughput microparticle synthesis. *Nat Mater* 2006;5(5):365-9
25. Gratton SE, Pohlhaus PD, Lee J, et al. Nanofabricated particles for engineered drug therapies: a preliminary biodistribution study of PRINT nanoparticles. *J Control Rel* 2007;121(1-2):10-8
26. Gratton SE, Napier ME, Ropp PA, et al. Microfabricated Particles for Engineered Drug Therapies: Elucidation into the Mechanisms of Cellular Internalization of PRINT Particles. *Pharm Res* 2008
27. Discher DE, Eisenberg A. Polymer vesicles. *Science* 2002;297(5583):967-73
28. Jain S, Bates FS. On the origins of morphological complexity in block copolymer surfactants. *Science* 2003;300(5618):460-4
29. Lee JC, Bermudez H, Discher BM, et al. Preparation, stability, and in vitro performance of vesicles made with diblock copolymers. *Biotechnol Bioeng* 2001;73(2):135-45
30. Dalhaimer P, Bates FS, Discher DE. Single molecule visualization of stable, stiffness-tunable, flow-conforming worm micelles. *Macromolecules* 2003;36(18):6873-7
31. Bermudez H, Brannan AK, Hammer DA, et al. Molecular weight dependence of polymersome membrane structure, elasticity, and stability. *Macromolecules* 2002;35(21):8203-8
32. Ahmed F, Discher DE. Self-porating polymersomes of PEG-PLA and PEG-PCL: hydrolysis-triggered controlled release vesicles. *J Control Release* 2004;96(1):37-53
33. Geng Y, Dalhaimer P, Cai S, et al. Shape effects of filaments versus spherical particles in flow and drug delivery. *Nat Nano* 2007;2(4):249-55
- **This paper demonstrates an unprecedented prolonged circulation profile of elongated filomicelles in animals.**
34. Simone EA, Dziubla TD, Colon-Gonzalez F, et al. Effect of polymer amphiphilicity on loading of a therapeutic enzyme into protective filamentous and spherical polymer nanocarriers. *Biomacromolecules* 2007;8(12):3914-21
- **This paper demonstrates the first successful loading of active therapeutic enzymes into elongated nanofilaments.**
35. Zheng LX, O'Connell MJ, Doorn SK, et al. Ultralong single-wall carbon nanotubes. *Nature Materials* 2004;3(10):673-6
36. Pampaloni F, Florin EL. Microtubule architecture: inspiration for novel carbon nanotube-based biomimetic materials. *Trends Biotechnol* 2008;26(6):302-10
37. Bianco A, Kostarelos K, Prato M. Opportunities and challenges of carbon-based nanomaterials for cancer therapy. *Expert Opin Drug Deliv* 2008;5(3):331-42
38. Zarif L. Drug delivery by lipid cochleates. *Methods Enzymol* 2005;391:314-29
39. Sharkey PK, Graybill JR, Johnson ES, et al. Amphotericin B lipid complex compared with amphotericin B in the treatment of cryptococcal meningitis in patients with AIDS. *Clin Infect Dis* 1996;22(2):315-21
40. Petros RA, Ropp PA, DeSimone JM. Reductively labile PRINT particles for the delivery of doxorubicin to HeLa cells. *J Am Chem Soc* 2008;130(15):5008-9
41. Kelly JY, DeSimone JM. Shape-specific, monodisperse nano-molding of protein particles. *J Am Chem Soc* 2008;130(16):5438-9
42. Liggins RT, Burt HM. Polyether-polyester diblock copolymers for the preparation of paclitaxel loaded polymeric micelle formulations. *Adv Drug Deliv Rev* 2002;54(2):191-202
43. Dalhaimer P, Engler AJ, Parthasarathy R, Discher DE. Targeted worm micelles. *Biomacromolecules* 2004;5(5):1714-9
44. Cai S, Vijayan K, Cheng D, et al. Micelles of Different Morphologies – Advantages of Worm-like Filomicelles of PEO-PCL in Paclitaxel Delivery. *Pharm Res* 2007;24(6):2099-109
45. Ahmed F, Pakunlu RI, Srinivas G, et al. Shrinkage of a rapidly growing tumor by drug-loaded polymersomes: pH-triggered release through copolymer degradation. *Mol Pharm* 2006;3(3):340-50
46. Accardo A, Tesaro D, Aloj L, et al. Peptide-containing aggregates as selective nanocarriers for therapeutics. *ChemMedChem* 2008;3(4):594-602
47. Hilder TA, Hill JM. Carbon nanotubes as drug delivery nanocapsules. *Curr Appl Phys* 2008;8(3-4):258-61
48. Popat KC, Eltgroth M, LaTempa TJ, et al. Titania nanotubes: a novel platform for drug-eluting coatings for medical implants? *Small* 2007;3(11):1878-81
49. Garnacho C, Dhami R, Simone EA, et al. Delivery of Acid Sphingomyelinase in Normal and Niemann-Pick Disease Mice Using Intercellular Adhesion Molecule-1-Targeted Polymer Nanocarriers. *J Pharmacol Exp Ther* 2008;325(2):400-8
- **This paper demonstrates the first successful targeted delivery of a therapeutic enzyme for the treatment of lysosomal storage disorders.**
50. Takagi A, Hirose A, Nishimura T, et al. Induction of mesothelioma in p53+/- mouse by intraperitoneal application of multi-wall carbon nanotube. *J Toxicol Sci* 2008;33(1):105-16

51. Tazawa H, Tatemichi M, Sawa T, et al. Oxidative and nitrate stress caused by subcutaneous implantation of a foreign body accelerates sarcoma development in Trp53<sup>+/−</sup> mice. *Carcinogenesis* 2007;28(1):191-8
52. Kumar N, Ravikumar MN, Domb AJ. Biodegradable block copolymers. *Adv Drug Deliv Rev* 2001;53(1):23-44
53. Shive MS, Anderson JM. Biodegradation and biocompatibility of PLA and PLGA microspheres. *Adv Drug Deliv Rev* 1997;28(1):5-24
54. Siepmann J, Gopferich A. Mathematical modeling of bioerodible, polymeric drug delivery systems. *Adv Drug Deliv Rev* 2001;48(2-3):229-47
55. Hanes J, Chiba M, Langer R. Synthesis and Characterization of Degradable Anhydride-co-imide Terpolymers Containing Trimellitylimido-L-Tyrosine: Novel Polym Drug Deliv Macromol 1996;29(16):5279-87
56. Leong KW, Brott BC, Langer R. Bioerodible polyanhydrides as drug-carrier matrices. I: Characterization, degradation, and release characteristics. *J Biomed Mater Res* 1985;19(8):941-55
57. Tabata Y, Gutta S, Langer R. Controlled delivery systems for proteins using polyanhydride microspheres. *Pharm Res* 1993;10(4):487-96
58. Jiang HL, Zhu KJ. Preparation, characterization and degradation characteristics of polyanhydrides containing poly(ethylene glycol). *Polym Int* 1999;48(1):47-52
59. Carino GP, Jacob JS, Mathiowitz E. Nanosphere based oral insulin delivery. *J Control Release* 2000;65(1-2):261-9
60. Fu J, Wu, Chi. Laser Light Scattering of the Degradation of Poly(sebacic anhydride) Nanoparticles. *Journal of Polymer Science : Part B: Polymer Physics* 2001;39(6):703-8
61. Pfeifer BA, Burdick JA, Langer R. Formulation and surface modification of poly(ester-anhydride) micro- and nanospheres. *Biomaterials* 2005;26(2):117-24
62. Li S, Garreau H, Vert M. Structure–property relationships in the case of the degradation of solid aliphatic poly-( $\alpha$ -hydroxy acids) in aqueous media part 3: influence of the morphology of poly(L-lactic acid). *J Mater Sci Mater Med* 1990;1(4):198-206
63. Li S, Garreau H, Vert M. Structure–property relationships in the case of the degradation of solid aliphatic poly-( $\alpha$ -hydroxy acids) in aqueous media. Part 1 Poly(DL-lactic acid). *J Mater Sci Mater Med* 1990;1(3):123
64. Duncan R. The dawning era of polymer therapeutics. *Nat Rev Drug Discov* 2003;2(5):347-60
65. Geng Y, Discher DE. Hydrolytic degradation of poly(ethylene oxide)-block-polycaprolactone worm micelles. *J Am Chem Soc* 2005;127(37):12780-1
66. Shih C. A graphical method for the determination of the mode of hydrolysis of biodegradable polymers. *Pharm Res* 1995;12(12):2036-60
67. Gopferich A. Mechanisms of polymer degradation and erosion. *Biomaterials* 1996;17(2):103-14
68. Li S, Molina I, Martinez MB, Vert M. Hydrolytic and enzymatic degradations of physically crosslinked hydrogels prepared from PLA/PEO/PLA triblock copolymers. *J Mater Sci Mater Med* 2002;13(1):81-6
69. MacDonald RT, McCarthy SP, Gross RA. Enzymatic degradability of poly(lactide): effects of chain stereochemistry and material crystallinity. *Macromolecules* 1996;29(23):7356-61
70. Tokiwa Y, Jarerat A. Biodegradation of poly(L-lactide). *Biotechnol Lett* 2004;26(10):771-7
71. Klibanov AL, Maruyama K, Torchilin VP, Huang L. Amphipathic polyethyleneglycols effectively prolong the circulation time of liposomes. *FEBS Lett* 1990;268(1):235-7
72. Lee JC, Wong DT, Discher DE. Direct measures of large, anisotropic strains in deformation of the erythrocyte cytoskeleton. *Biophys J* 1999;77(2):853-64
73. Moghimi SM, Porter CJ, Muir IS, et al. Non-phagocytic uptake of intravenously injected microspheres in rat spleen: influence of particle size and hydrophilic coating. *Biochem Biophys Res Commun* 1991;177(2):861-6
74. Singh R, Pantarotto D, Lacerda L, et al. Tissue biodistribution and blood clearance rates of intravenously administered carbon nanotube radiotracers. *Proc Natl Acad Sci USA* 2006;103(9):3357-62
75. Liu Z, Davis C, Cai W, et al. Circulation and long-term fate of functionalized, biocompatible single-walled carbon nanotubes in mice probed by Raman spectroscopy. *Proc Natl Acad Sci USA* 2008;105(5):1410-5
76. Lacerda L, Ali-Boucetta H, Herrero MA, et al. Tissue histology and physiology following intravenous administration of different types of functionalized multiwalled carbon nanotubes. *Nanomedicine* 2008;3(2):149-61
77. Bedu-Addo FK, Tang P, Xu Y, Huang L. Interaction of polyethyleneglycol–phospholipid conjugates with cholesterol–phosphatidylcholine mixtures: sterically stabilized liposome formulations. *Pharm Res* 1996;13(5):718-24
78. Cato MH, D'Annibale F, Mills DM, et al. Cell-type specific and cytoplasmic targeting of PEGylated carbon nanotube-based nanoassemblies. *J Nanosci Nanotechnol* 2008;8(5):2259-69
79. McDevitt MR, Chattopadhyay D, Kappel BJ, et al. Tumor targeting with antibody-functionalized, radiolabeled carbon nanotubes. *J Nucl Med* 2007;48(7):1180-9
80. Garnacho C, Albelda SM, Muzykantov VR, Muro S. Differential intra-endothelial delivery of polymer nanocarriers targeted to distinct PECAM-1 epitopes. *J Control Release* 2008;130(3):226-33
81. Muzykantov VR. Targeting pulmonary endothelium. In: Muzykantov VR, et al, editor. *Biomedical aspects of drug targeting*. Boston: Kluwer Academic Publishers; 2003. p. 129-48
82. Lamaze C, Schmid SL. The emergence of clathrin-independent pinocytic pathways. *Curr Opin Cell Biol* 1995;7(4):573-80
83. Hewlett LJ, Prescott AR, Watts C. The coated pit and macropinocytic pathways serve distinct endosome populations. *J Cell Biol* 1994;124(5):689-703
84. Koval M, Preiter K, Adles C, et al. Size of IgG-opsonized particles determines macrophage response during internalization. *Exp Cell Res* 1998;242(1):265-73
85. Storrie B, Desjardins M. The biogenesis of lysosomes: is it a kiss and run, continuous fusion and fission process? *Bioessays* 1996;18(11):895-903
86. Brewer JM, Tetley L, Richmond J, et al. Lipid vesicle size determines the Th1 or Th2 response to entrapped antigen. *J Immunol* 1998;161(8):4000-7
87. Romero EL, Morilla MJ, Regts J, et al. On the mechanism of hepatic transendothelial



- passage of large liposomes. FEBS Lett 1999;448(1):193-6
88. Champion JA, Mitragotri S. Shape Induced Inhibition of Phagocytosis of Polymer Particles. Pharm Res 2008 [Epub ahead of print]
89. Caron E, Hall A. Phagocytosis: Oxford University Press, 2001
90. Sahagian GG, Steer CJ. Transmembrane orientation of the mannose 6-phosphate receptor in isolated clathrin-coated vesicles. J Biol Chem 1985;260(17):9838-42
91. Muro S, Wiewrodt R, Thomas A, et al. A novel endocytic pathway induced by clustering endothelial ICAM-1 or PECAM-1. J Cell Sci 2003;116(Pt 8):1599-609
92. Kok RJ, Everts M, Asgeirsdottir SA, et al. Cellular handling of a dexamethasone-anti-E-selectin immunoconjugate by activated endothelial cells: comparison with free dexamethasone. Pharm Res 2002;19(11):1730-5
93. Ricard I, Payet MD, Dupuis G. VCAM-1 is internalized by a clathrin-related pathway in human endothelial cells but its alpha 4 beta 1 integrin counter-receptor remains associated with the plasma membrane in human T lymphocytes. Eur J Immunol 1998;28(5):1708-18
94. Tsourkas A, Shinde-Patil VR, Kelly KA, et al. In vivo imaging of activated endothelium using an anti-VCAM-1 magnetooptical probe. Bioconjug Chem 2005;16(3):576-81
95. Finger VH, Taber SW, Buschemeyer WC, et al. Constitutive and stimulated expression of ICAM-1 protein on pulmonary endothelial cells in vivo. Microvasc Res 1997;54(2):135-44
96. Kam NW, Liu Z, Dai H. Carbon nanotubes as intracellular transporters for proteins and DNA: an investigation of the uptake mechanism and pathway. Angew Chem Int Ed Engl 2006;45(4):577-81
97. Jin H, Heller DA, Strano MS. Single-Particle Tracking of Endocytosis and Exocytosis of Single-Walled Carbon Nanotubes in NIH-3T3 Cells. Nano Lett 2008;8(6):1577-85
98. Kostarelos K, Lacerda L, Pastorin G, et al. Cellular uptake of functionalized carbon nanotubes is independent of functional group and cell type. Nat Nanotechnol 2007;2(2):108-13
99. Beningo KA, Wang YL. Fc-receptor-mediated phagocytosis is regulated by mechanical properties of the target. J Cell Sci 2002;115(Pt 4):849-56.

## Affiliation

Eric A Simone<sup>†1,2,3</sup>, Thomas D Dziubla<sup>2,4</sup> & Vladimir R Muzykantov<sup>†1,2,3,5</sup>

<sup>†</sup>Author for correspondence

<sup>†1</sup>University of Pennsylvania, Department of Bioengineering, 3620 Hamilton Walk, 1 John Morgan Building, Philadelphia, PA 19104, USA  
Tel: +1 215 898 9823; Fax: +1 215 898 0868;  
E-mail: muzykant@mail.med.upenn.edu (enzyme therapeutics)

<sup>2</sup>University of Pennsylvania, Institute for Translational Medicine and Therapeutics, Philadelphia, PA 19104, USA

<sup>3</sup>University of Pennsylvania School of Medicine, Institute for Environmental Medicine, Philadelphia, PA 19104, USA

<sup>4</sup>University of Kentucky, Department of Chemical and Materials Engineering, Lexington, KY 40506, USA

<sup>5</sup>University of Pennsylvania School of Medicine, Department of Pharmacology, Philadelphia, PA 19104, USA